Reprinted from

CMES

Computer Modeling in Engineering & Sciences

Founder and Editor-in-Chief:
Satya N. Atluri

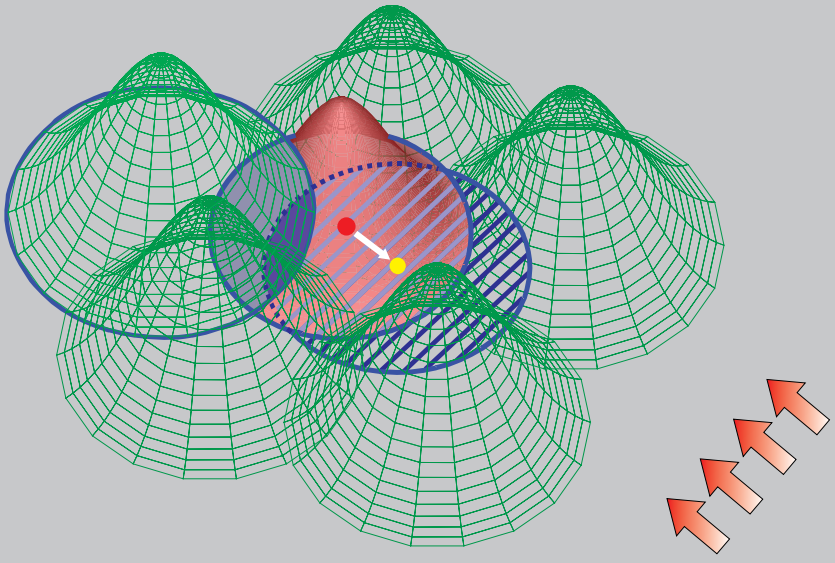

ISSN: 1526-1492 (print)
ISSN: 1526-1506 (on-line)

Tech Science Press

Copyright © 2010 Tech Science Press CMES, vol.66, no.2, pp.165-185, 2010

Representative Volume Element Size of Elastoplastic and Elastoviscoplastic Particle-Reinforced Composites with Random Microstructure

J. Cugnoni[1] **and M. Galli**[2]

Abstract: With the progress of miniaturization, in many modern applications the characteristic dimensions of the physical volume occupied by particle-reinforced composites are getting comparable with the reinforcement size and many of those composite materials undergo plastic deformations. In both experimental and modelling contexts, it is therefore very important to know whether, and up to which characteristic size, the description of the composites in terms of effective, homogenized properties is sufficiently accurate to represent their response in the actual geometry. Herein, the case of particle-reinforced composites with elastoviscoplastic matrix materials and polyhedral randomly arranged linear elastic reinforcement is considered since it is representative of many metal matrix composites of technical interests. A large parametric study based on 3D finite element microstructural models is carried out to study the dependence of the Representative Volume Element (RVE) size on the mechanical properties of the constituents, the reinforcement volume fraction and the average strain level. The results show that RVE size mainly depends on the reinforcement volume fraction and on the macroscopic strain level. The estimated RVE size for elastoplastic composites with 5% to 10% volume fraction of reinforcements is found in the range of 5-6 times the average size of reinforcement particles, while for higher volume fraction, *e.g.* 15% to 25%vol., the RVE size increases rapidly to 10 to 20 times the reinforcement size. Moreover insights on the influence of mesh refinement and boundary conditions on finite element homogenization analysis are obtained.

Keywords: Homogenization, Mesh Refinement, RVE, Elastoplastic, Viscoplastic.

[1] Laboratoire de Mécanique Appliquée et d'analyse de Fiabilité, École Polytechnique Fédérale Lausanne, Lausanne, 1015, Switzerland

[2] Engineering Department, University of Cambridge, Trumpington St., Cambridge, CB2 1PZ, UK

1 Introduction

A fundamental concept when studying composite materials is that of Representative Volume Element (RVE). Among the different definitions of this entity (Nemat-Nasser and Hori, 1993) that by Drugan and Willis (1996) is particularly appropriate for this work: the RVE is 'the smallest material volume element of the composite for which the usual spatially constant macroscopic representation is a sufficiently accurate model to represent mean constitutive response'. This very pragmatic definition implies that random media have a finite RVE whose dimensions vary as a function of the desired accuracy. In this context it is useful to introduce the concept of mesoscale which is the characteristic lengthscale of the RVE. Moreover the application of this definition requires the assessment of the error made when interpreting the composite mechanical response as it were a homogeneous material and the actual constitutive behavior with the objective of ascertaining if the approximation is 'sufficiently accurate'. In this sense Drugan and Willis (1996) show that, for linear elastic composites, a mesoscale model or sample of approximately twice the characteristic reinforcement diameter is sufficient to limit the error to 5% while the required size increases to approximately 4.5 times the characteristic reinforcement diameter to have an error of 1%. When elastoviscoplastic composites are considered, larger mesoscale volumes are required to reach similar levels of accuracy because of the higher levels of inhomogeneity in the strain field caused by the development of plastic strain concentrations.

During the last ten years significant progress has been made in the development of mesoscale finite element (FE) models which can provide representative effective elastoviscoplastic responses for isotropic random particle-reinforced composites (McDowell, 2010). Because of the importance of stress triaxiality, homogenization FE models must be three-dimensional (Böhm and Han, 2001) to provide reliable estimates of the response of random particle-reinforced composites. As a consequence of the high computational cost of such three dimensional FE models, the research has mostly been focused on the development of periodic multi-inclusion unit cells with spherical reinforcement (Böhm et al., 2004; Gonzalez et al., 2004; Pierard et al., 2007) to predict the representative effective elasto-plastic response of composites. Assuming periodicity of the microstructure significantly helps to minimize the required mesoscale volume, and therefore the computational cost, since periodic boundary conditions tend to reduce the sensitivity of the simulations to localization problems. Moreover, considering spherical particles also helps to reduce the mesoscale volume as the reinforcement shape does not induce any anisotropy in the composite. Although these periodic models can provide accurate estimates of the effective medium response they cannot yield the dimensions of the RVE in Drugan and Willis' sense, since random particle-reinforced composites are not

periodic and their response strongly depends on plastic strain concentrations and therefore on the reinforcement spatial distribution (Ostoja-Starzewski, 2005). The availability of such information is very important for both the experimental and the modeling activity in technological applications where relatively limited volumes of composite are utilized, *e.g.* reinforced solder and brazing alloys (Sivasubramanian et al., 2009; Galli et al., 2006) or functionally graded interface layers (Shabana and Noda, 2002).

In the present work a large scale parametric FE homogenization study was carried out with the objective of obtaining estimates of the physical size of the RVE of a broad range of elastoplastic and elastoviscoplastic random particle-reinforced composites. The simulations were carried out under mixed static-kinematic uniform boundary conditions which are representative of the actual configuration of the composites in many applications and experiments. To estimate the RVE, FE simulations were carried out on increasingly larger three dimensional mesoscale models until convergence of the effective response was achieved. Moreover different levels of mesh refinement and sets of boundary conditions were considered in order to assess the influence of these parameters on the RVE size.

2 Methods

2.1 Microstructure and Mesh

The FE models of particle-reinforced composites were created using the approach developed by Galli et al. (2008), which allows for the fast generation of three dimensional mesoscale cubic domains. The procedure consists of 3 main steps:

1. A cubic domain is discretized by means of the TetGen software (Si , 2009) which performs a constrained Delaunay tetrahedralization which respects the domain boundary and has among its vertices a set of randomly generated points.

2. Particles are created sequentially by assigning the inclusion material properties to all the tetrahedra sharing randomly selected vertices. If a particle shares a face with an already existent one or its volume is not in the prescribed range, it is discarded. The procedure is iterative and ends once the prescribed reinforcement volume fraction is achieved.

3. The mesh is refined by performing a second constrained Delaunay tetrahedralization which respects not only the domain boundary but also the interface between matrix and particles. The actual mesh refinement is obtained by imposing the value of the maximum admissible element volume.

For a more extensive description of the procedure the reader is referred to the work by Galli et al. (2008). Five different reinforcement volume fractions V_R were considered: 0.05, 0.10, 0.15, 0.20 and 0.25. In the following the five composites are indicated as 'p05', 'p10', 'p15', 'p20' and 'p25', for the sake of brevity. For all the compositions five mesoscale models of increasing dimensions were generated, with the ratios of the larger volumes to the smallest being 8, 27, 64 and 125, respectively. Again, for the sake of brevity, in the following the five volumes are indicated as 'v1', 'v2', 'v3', 'v4' and 'v5'. Following Galli et al. (2008) the model size was measured with respect to the particle dimension by using the metric ξ:

$$\xi = \sqrt[3]{\frac{V}{V_P}}, \tag{1}$$

where V is the volume of the model and V_P the average particle volume. Three different levels of mesh refinement were considered: the coarser mesh was that obtained from the original tetrahedralization, with no refinement, while for the finer meshes constraints on the maximum element volume were imposed. Analogously to the other features of the models, in the following the three mesh refinement levels are indicated as 'r1', 'r2' and 'r3', respectively. The main geometrical and mesh-related features of the models are summarized in table 1. Some example meshes are shown in figure 1. The differences between the levels of mesh refinement can be appreciated by examining the evolution of the numbers of nodes and elements, N_N and N_E, respectively, for $\xi = 4.64$ in table 1. If the model with 5% volume fraction is considered, it can be seen that the N_N approximately quadruplicates from mesh refinement level r1 to r2 and doubles from r2 to r3. The three corresponding meshes are shown in the left column of figure 1: a) v1p05r1, b) v1p05r2 and c) v1p05r3. If the mesh on the particle surfaces is considered it can be seen that in the case of r2 each triangular facet is discretized with approximately 3 to 6 elements while for r3 this figure increases to approximately 7 to 14. The dimensional range of the models considered in the study is well illustrated by comparing the number of particles N_P for the same reinforcement volume fraction V_R for different values of ξ in table 1: N_P in the largest models is approximately 100 times larger than in the smallest. This can also be appreciated by comparing figure 1 c) and f): for $V_R = 0.05$ the smallest mesoscale volume contains 6 particles while the largest 661. The three dimensional view also helps to quantify the reinforcement density: the three meshes in the right column of figure 1, d) v5p05r1, e) v3p15r1, f) v2p25r1 are characterized by different values of reinforcement volume fraction. It can be noted how densely reinforced p25 composites are. Actually, their reinforcement volume fraction, 0.25, is close to the jamming limit of the algorithm which generates the particle distribution, approximately 0.26 (Galli et al., 2008).

The FE models were solved using ABAQUS (version 6.8, Simulia, Providence, RI, USA). Ten-node modified quadratic elements were employed to avoid possible volumetric locking in yielded regions. Simulations were carried out under the small deformation assumption. For the elastoplastic simulations the domain decomposition iterative linear equation solver was employed to minimize the computational time. In the case of the elastoviscoplastic simulations the default direct sparse solver was used and a value of 1E-3 was chosen for the maximum admissible difference in the creep strain increment calculated from the creep strain rates based on conditions at the beginning and on conditions at the end of a time increment.

2.2 Boundary Conditions

The uniaxial response of a material with random microstructure can be simulated by using four different sets of boundary conditions. When considering a mesoscale cube with edge length L, one vertex in the origin and the others in the first octant ($x_i \in [0,L]^3$), the boundary conditions for tension or compression in the x_1 direction can be written as:

$$\begin{cases} t_1(0,x_2,x_3) = -\overline{\sigma} \\ t_1(L,x_2,x_3) = \overline{\sigma} \\ t_2(x_1,0,x_3) = 0 \\ t_2(x_1,L,x_3) = 0 \\ t_3(x_1,x_2,0) = 0 \\ t_3(x_1,x_2,L) = 0 \end{cases} \tag{2}$$

$$\begin{cases} u_1(0,x_2,x_3) = 0 \\ u_1(L,x_2,x_3) = \overline{\varepsilon}L \\ t_2(x_1,0,x_3) = 0 \\ t_2(x_1,L,x_3) = 0 \\ t_3(x_1,x_2,0) = 0 \\ t_3(x_1,x_2,L) = 0 \end{cases} \tag{3}$$

Table 1: Main features of the FE mesoscale models used in the parametric study: ξ, characteristic size defined according to (1); V_R, reinforcement volume fraction; N_P number of particles; r1, r2, r3, different levels of mesh refinement (see section 2.1); N_N number of nodes; N_E number of elements.

ξ	V_R	N_P	Name	Mesh refinement					
				r1		r2		r3	
				N_N	N_E	N_N	N_E	N_N	N_E
4.64	0.05	6	v1p05	4.9E3	3.1E3	2.1E4	1.1E4	3.8E4	2.4E4
	0.10	13	v1p10	4.9E3	3.1E3	2.7E4	1.6E4	4.4E4	2.8E4
	0.15	19	v1p15	4.9E3	3.1E3	3.4E4	2.1E4	5.2E4	3.4E4
	0.20	29	v1p20	4.9E3	3.1E3	4.1E4	2.6E4	5.7E4	3.7E4
	0.25	36	v1p25	4.9E3	3.1E3	5.6E4	3.7E4	7.0E4	4.7E4
9.30	0.05	47	v2p05	3.3E4	2.3E4	1.4E5	8.3E4	-	-
	0.10	94	v2p10	3.3E4	2.3E4	2.1E5	1.3E5	-	-
	0.15	146	v2p15	3.3E4	2.3E4	2.6E5	1.7E5	-	-
	0.20	196	v2p20	3.3E4	2.3E4	3.4E5	2.3E5	-	-
	0.25	248	v2p25	3.3E4	2.3E4	4.2E5	2.9E5	-	-
13.9	0.05	153	v3p05	1.1E5	7.6E4	4.7E5	2.8E5	-	-
	0.10	302	v3p10	1.1E5	7.6E4	6.8E5	4.4E5	-	-
	0.15	459	v3p15	1.1E5	7.6E4	9.1E5	6.1E5	-	-
	0.20	614	v3p20	1.1E5	7.6E4	1.2E6	8.1E5	-	-
	0.25	781	v3p25	1.1E5	7.6E4	1.5E6	1.0E6	-	-
18.6	0.05	352	v4p05	2.5E5	1.8E5	-	-	-	-
	0.10	687	v4p10	2.5E5	1.8E5	-	-	-	-
	0.15	1054	v4p15	2.5E5	1.8E5	-	-	-	-
	0.20	1427	v4p20	2.5E5	1.8E5	-	-	-	-
	0.25	1814	v4p25	2.5E5	1.8E5	-	-	-	-
23.2	0.05	661	v5p05	4.8E5	3.5E5	-	-	-	-
	0.10	1341	v5p10	4.8E5	3.5E5	-	-	-	-
	0.15	2037	v5p15	4.8E5	3.5E5	-	-	-	-
	0.20	2734	v5p20	4.8E5	3.5E5	-	-	-	-
	0.25	3463	v5p25	4.8E5	3.5E5	-	-	-	-

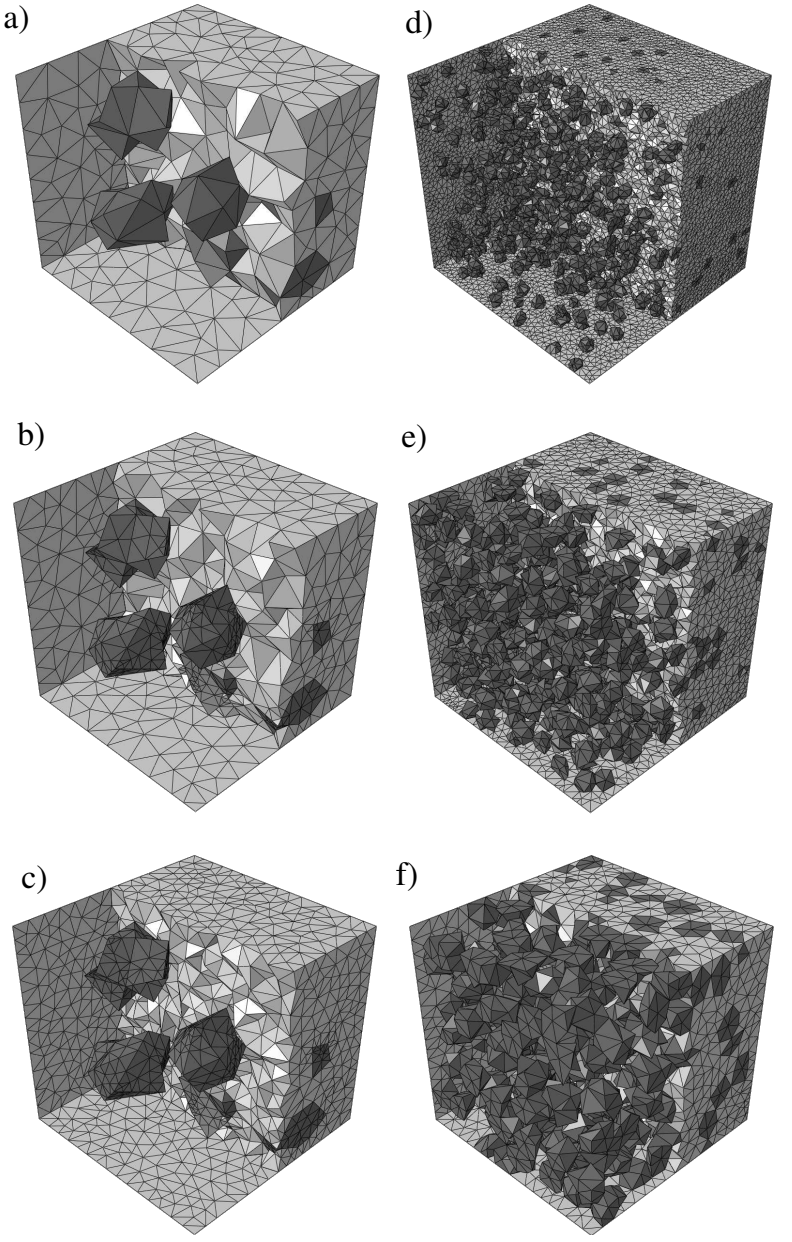

Figure 1: Six illustrative examples of the mesoscale FE models (part of the matrix material elements are not displayed): a) v1p05r1, b) v1p05r2, c) v1p05r3, d)v5p05r1, e)v3p15r1, f) v2p25r1. Refer to sections 2.1 and 2.3 for the meaning of abbreviations.

$$\begin{cases} t_1(0,x_2,x_3) = -\overline{\sigma} \\ t_1(L,x_2,x_3) = \overline{\sigma} \\ u_2(x_1,0,x_3) = 0 \\ u_2(x_1,L,x_3)\,|_{x_2,x_3\neq L} = u_2(0,L,L) \\ u_3(x_1,x_2,0) = 0 \\ u_3(x_1,x_2,L)\,|_{x_2,x_3\neq L} = u_3(0,L,L) \end{cases} \tag{4}$$

$$\begin{cases} u_1(0,x_2,x_3) = 0 \\ u_1(L,x_2,x_3) = \overline{\varepsilon}L \\ u_2(x_1,0,x_3) = 0 \\ u_2(x_1,L,x_3)\,|_{x_2,x_3\neq L} = u_2(0,L,L) \\ u_3(x_1,x_2,0) = 0 \\ u_3(x_1,x_2,L)\,|_{x_2,x_3\neq L} = u_3(0,L,L) \end{cases} \tag{5}$$

where εL and t_i are the imposed displacement and stress in the x_i direction. Boundary conditions (2) and (3) correspond to load- and displacement-controlled experiments, in which load or displacement is imposed in the tension-compression direction while the specimen lateral surface is stress-free. The other two sets, (4) and (5), correspond to load controlled and displacement controlled uniaxial tests in which the planarity of the faces parallel to the tensile direction is imposed as well. They have no direct experimental counterpart, nevertheless they can describe the response of a material rather than that of a single specimen (*e.g.* inside a structure much larger than the volume element). Note that set (5) can also be seen as describing a special case of microstructure, in which a volume element eight times the size of the original cell repeats periodically.

In the case of a homogeneous material all the sets of boundary conditions would lead to the same uniaxial stress-strain curve, independently of the size of the model. Following the classification by Jiang et al. (2001), set (2) corresponds to purely static uniform boundary conditions

$$t_i = \sigma_{ij} n_j \;\; \forall x_{ij} \in \partial\Omega, \tag{6}$$

set (5) to purely kinematic uniform boundary

$$u_i = \overline{\varepsilon}_{ij} x_j \;\; \forall x_{ij} \in \partial\Omega, \tag{7}$$

while the other two are mixed static-kinematic uniform boundary conditions

$$(t_i - \sigma_{ij} n_j)(u_i - \overline{\varepsilon}_{ij} x_j) = 0 \;\; \forall x_{ij} \in \partial\Omega. \tag{8}$$

In the present work, each set of boundary conditions was first tested in a separate parametric study in order to evaluate its influence on the predictions of effective elasto-plastic response and on the convergence of the volume of interest towards the RVE. In the second part of the work dedicated to the evaluation of the RVE size, only mixed static-kinematic boundary conditions (3) were used. Note that boundary conditions (2) and (3) are computationally less expensive than (4) and (5) since they do not impose any constraints on the displacements perpendicular to the load direction. As discussed in the introduction, periodic boundary conditions are usually preferred for the prediction of mean effective response but cannot provide good estimates of the physical RVE size of random particle reinforced composites and are thus not considered here.

2.3 Material Properties

For both the elastoplastic and the elastoviscoplastic simulations the inclusion material was assumed linear elastic with a Young's modulus E_P five times that of the matrix E_M while the same Poisson's ratio, 0.3, was assigned to the two materials. In the elatoplastic simulations the matrix material was assumed to be elastoplastic and to follow the Von Mises yield criterion with an isotropic bilinear hardening of the form

$$\begin{aligned} \sigma_y(\varepsilon_p) &= \sigma_y^0 + h\varepsilon_p/0.05 \quad && 0 \leq \varepsilon_p < 0.05 \\ \sigma_y(\varepsilon_p) &= \sigma_y^0 + h && \varepsilon_p \geq 0.05, \end{aligned} \tag{9}$$

where σ_y is the yield stress, ε_p the equivalent plastic strain and h the hardening coefficient. For σ_y the value $E_M/1000$ was chosen. Three different values of h were considered: 0, $0.2\sigma_y$ and $0.4\sigma_y$. In the following these three materials are referred to as 'h0', 'h2', 'h4'.

In the elastoviscoplastic simulations the matrix material was assigned a power law creep viscoplastic response:

$$\dot{\varepsilon}_{vp} = A\sigma^n \tag{10}$$

where $\dot{\varepsilon}_{vp}$ is the equivalent viscoplastic strain rate and σ is the equivalent von Mises stress. The proportionality coefficient A was kept constant while two values of the stress exponent $n = 4$ and $n = 8$ were considered. In the following these two materials are referred to as 'n4', 'n8'.

For the sake of the generality of the results, the effective stress-strain curves of the composites will be represented in a normalized form (section 3). For elastoplasticity, stress values are normalized by the yield stress of the matrix material σ_y^0 and strain values by the corresponding yield strain σ_y^0/E_m. For the normalization

of the elastoviscoplastic stress-strain curves an analogous strategy is used: stress values are divided by the yield stress of the matrix material at imposed strain rate $\sigma_{vp}^0 = (\dot{\bar{\varepsilon}}/A)^{(1/n)}$, strain values by the corresponding yield strain $\varepsilon_{vp}^0 = \sigma_{vp}^0/E_M$.

2.4 Representativeness Metric

According to the definition by Drugan and Willis (1996) the RVE size is achieved when the effective mesoscale response is sufficiently accurate. Considering the simulated stress-strain response of the largest mesoscale model (namely 'v5' with ξ_{max}=23.2) as a reference, the relative cumulative error norm R is proposed as representativeness metric

$$R(\bar{\varepsilon},\xi) = \frac{\int_0^{\bar{\varepsilon}} |\sigma(\varepsilon',\xi) - \sigma(\varepsilon',\xi_{max})| d\varepsilon'}{\int_0^{\bar{\varepsilon}} \sigma(\varepsilon',\xi_{max}) d\varepsilon'}, \tag{11}$$

where $\bar{\varepsilon}$ is the imposed average strain level and σ and ε are the volumetric average values of the stress and strain components in the tensile direction. Note that this error function R represents a surface of relative prediction error as a function of the total applied strain $\bar{\varepsilon}$ and the size of the simulated mesoscale volume ξ. Therefore, given a maximum relative error threshold, the size of the RVE can be estimated by finding the smallest mesoscale volume for which the cumulative error norm is below the chosen error threshold value. In the present work, a maximum error value of 2% was chosen and bilinear interpolation was used to approximate the error surface from the discrete FE simulation results.

3 Results and Discussion

3.1 Effect of Boundary Conditions

The results of the parametric study dedicated to the influence of the boundary conditions are summarized in figure 2. It can be noted that with purely static boundary conditions (2) only very limited effective strain levels could be obtained. The nonlinear FE solver could not converge because of significant plastic strain localization in the corners of the mesoscale models. This problem clearly shows that purely stress-based boundary conditions are inappropriate for the homogenization of plastic materials as they do not sufficiently constrain the development of the plastic field and yield to premature localization in the corner regions of the model. On the other hand the other three sets of boundary conditions did not suffer from any numerical problem. Nevertheless, the macroscopic response obtained with kinematic boundary conditions (5) despite converging to a unique stress-strain curve for larger mesoscale volumes, overestimates the stiffness of the composite since the imposed planarity of all the boundary faces strongly prevents the development of plastic

deformation near the boundaries of the mesoscale volume. Therefore an upper estimate of the effective response of the medium is obtained. The two sets of mixed boundary conditions (3) and (4) clearly exhibit convergence to the same response for increasing mesoscale volumes. As expected, the converged predictions of the stress-strain curve obtained with hybrid boundary conditions predict significantly smaller stress values than those obtained by applying (5). Note that the stiffness of the obtained response is proportional to the number of faces of the mesoscale volume which are constrained to stay planar during deformation: none for (2), two for (2), four for (4) and all the six faces for (5). These results confirm those formerly obtained by Jiang et al. (2001), Ostoja-Starzewski (2008) and Galli et al. (2008) and show that similarly to linear elasticity the stiffness of the obtained response is proportional to the number of faces which keep planar during the deformation process (Huet, 1997). If progressively larger volumes of material are considered the difference between the curves obtained with the same set of boundary conditions decreases. The first two sets of boundary conditions whose responses become constant with ξ are (3) and (4) moreover the differences between the respective stress strain curves are negligible, therefore the RVE size is achieved.

The results of the study of the influence of boundary conditions support the choice of adopting mixed boundary conditions (3) throughout the rest of the work. Comparisons with experiments (Sivasubramanian et al., 2009) show that hybrid boundary conditions usually tend to provide more realistic estimates of the overall response of elastoplastic composites as they do not excessively constrain the development of plastic strain in the model. The choice of mixed uniform boundary conditions is in line with the results by Jiang et al. (2001), who studied the shear response of an elastoplastic random composite under mixed boundary conditions. Moreover Pahr and Böhm (2008) validated the applicability of mixed boundary conditions for assessment of the elastoplastic response of orthotropic composites. The present results also confirms those obtained in the case of linear elasticity with and without damage (Huet, 1997; Pahr and Zysset, 2008).

After this study on the influence of boundary conditions on the composite response, all the subsequent results in the present work were obtained by applying mixed boundary conditions (3). Note that for homogenization studies, that is to say with the objective of assessing effective properties, the use of periodic boundary conditions is in general preferred, *e.g.* Böhm and Han (2001); Pierard et al. (2007), since compared to purely static or kinematic boundary conditions they provide a sufficiently accurate effective behaviour with smaller unit cells. However, to the authors' knowledge a rigorous comparative study on their computational performance compared with that of boundary conditions (3), (4) (5) is not reported in the literature. Moreover periodic boundary conditions require mesh periodicity and in

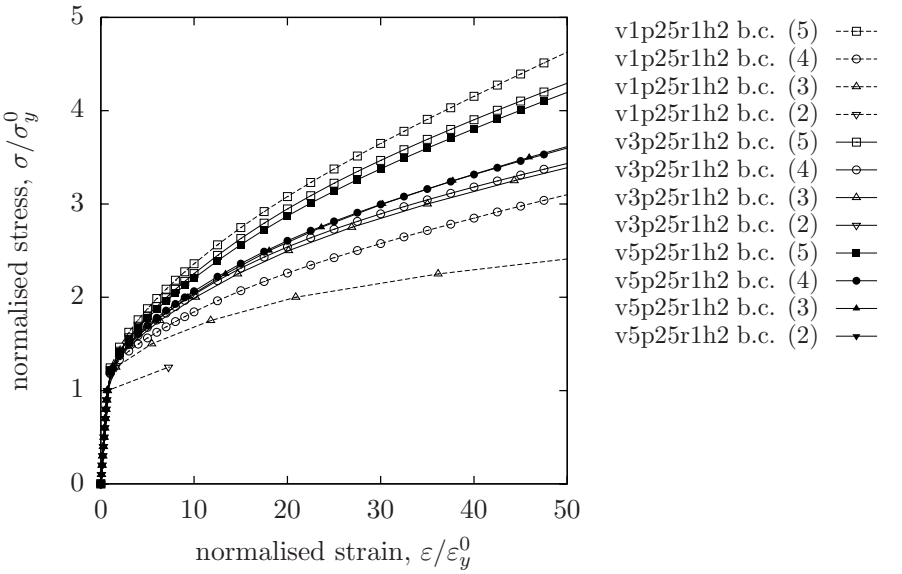

Figure 2: The influence of boundary conditions (b.c.) on the effective elastoplastic stress-strain curve: purely kinematic b.c. (5) lead to an overestimation of the effective stiffness; mixed b.c. (3) and (4) lead to the same stress-strain curve as larger volumes are considered (v3 and v5); the solution diverges for small normalised strain values when purely static b.c. (2) are applied. See table 1 for the model main features and sections 2.1 and 2.3 for the abbreviations.

general, *e.g.* for spherical inclusions, microstructure periodicity, which is not an applicable assumption for random particle reinforced composites as studied herein.

3.2 Mesh Convergence

Some significant results which illustrate the influence of mesh refinement on the effective properties are displayed in figure 3. It can be seen, figure 3 a), that for small volume fractions, p05, coarse meshes are already sufficient to catch the material response: both in elastoplasticity and elastoviscoplasticity the curves for r1, r2 and r3 are superposed. On the contrary, for higher reinforcement volume fractions mesh refinement is fundamental to get accurate results. As the volume fraction increases, the interaction distance between particles gets smaller and thus a finer mesh is required to capture the development of plastic deformation between particles. For this reason the responses for r2 and r3 are significantly more compliant than for r1. Moreover in all cases the difference between the stress-strain curves for r2 and r3 is negligible proving that the level of refinement r2, corresponding to approximately

225 elements per particle, is sufficient to obtain converged FE solutions. Figure 3 b) summarizes some of the results of the study of the influence of mesh refinement on the convergence of the mesoscale models towards the RVE. The relative differences between the stress-strain curves obtained with models of different dimensions, v1, v2 and v3, is approximately the same for refinement r1 and r2. Note that v3 is representative for the level of strain considered, therefore mesoscale models with r1 and r2 mesh refinements become representative for the same values of ξ. This leads to the important conclusion that in the considered framework – small strain and non-softening material response (Gitman et al., 2007) – the level of mesh refinement does not significantly affect the estimation of the RVE size. Nevertheless it is of paramount importance to obtain quantitatively accurate predictions of the effective stress-strain response of the elastoplastic or elastoviscoplastic composites. This result concurs with the findings by Li and Ostoja-Starzewski (2006) and supports the choice of using the first level of mesh refinement r1, computationally more affordable, to assess the RVE size throughout the rest of the study.

3.3 RVE size

An example of the obtained results for the relative error R as a function of strain is reported in figure 4 where the elastoplastic composite p15h2 is considered. The chosen error threshold is 0.02. It can be seen that v3 is representative up to an average strain of approximately 0.02 while if the level of deformation of interest is larger v4 is required.

The plots of the evolution of the RVE size with the effective strain are summarized in figures 5 and 6 for elastoplastic and elastoviscoplastic composites, respectively. In the following the influence of composition, material properties and strain magnitude, on the size of the RVE will be analysed individually with the objective of assessing their relative importance.

The RVE sizes of all the composites with the exception of those with 5% reinforcement volume fraction exhibit a strong dependence on the imposed effective strain. As the imposed macroscopic strain increases, already at effective stress levels well below the yield stress of the matrix material, plastic strain develops because of the stress concentrations due to the difference in the elastic properties of matrix and particles. The resulting strain field is highly inhomogeneous and large mesoscale volumes are required to obtain a representative average response. This effect is less evident in the composites with low reinforcement volume fraction because particles are almost isolated and therefore a nearly homogeneous strain field develops in most of the mesoscale volume.

If composition is considered, *i.e.* the reinforcement volume fraction, it can be observed that the size of the RVE is strongly related to the reinforcement volume

a)

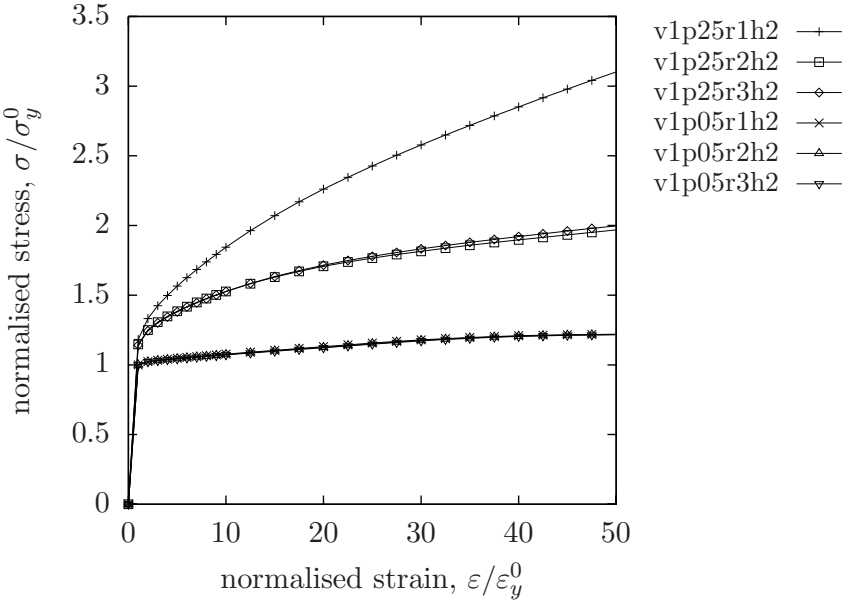

b)

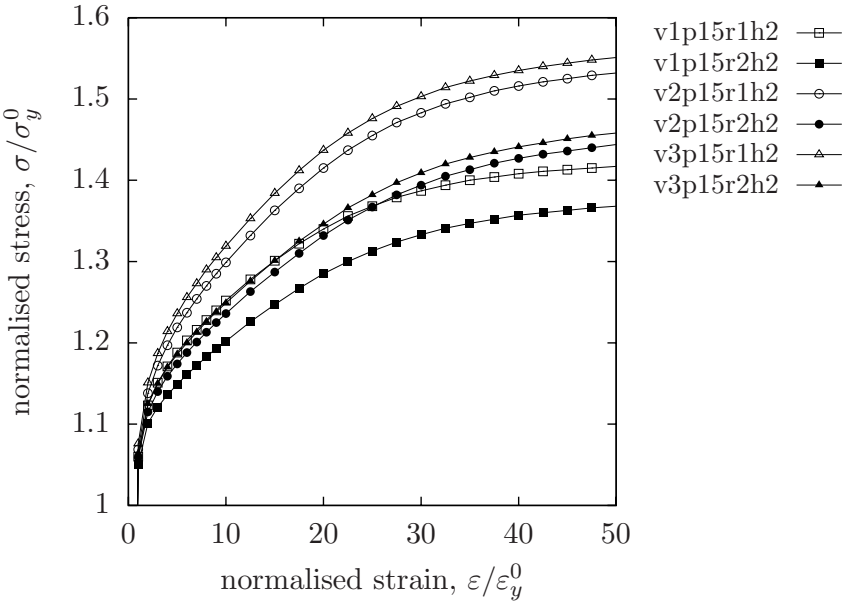

Figure 3: Study of the mesh convergence. Mesh refinement level r2 is required for composites with a reinforcement volume fraction larger than 5%, a). In b) it can be noted that the different models exhibit very similar shifts in the stress-strain curves due to mesh refinement.

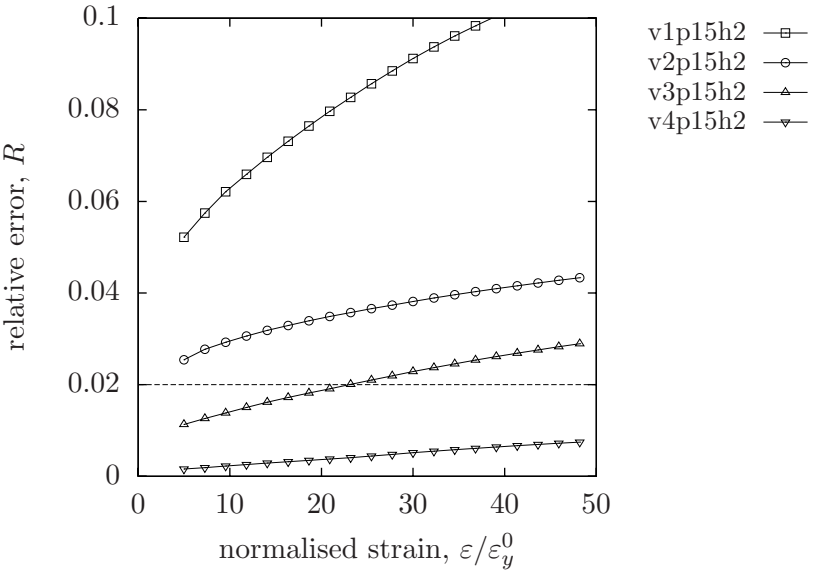

Figure 4: An example plot of the evolution of the relative error R, defined in (11), for an elastoplastic composite with 15% vol. reinforcement. The simulated volume is considered representative if $R \leq 0.02$.

fraction and this dependence is nontrivial. The RVE size for composites with 5% vol. reinforcement is in the interval $5 < \xi < 6$ for all the materials, therefore close to the value $\xi = 4.5$ reported by Drugan and Willis (1996) to have a 1% error for linear elastic composites. As the reinforcement volume fraction increases the size of the RVE becomes significantly larger and its dependence on strain more marked. It can be noted that the RVE size increases up to 20% vol. reinforcement and then decreases, with the 25% vol. reinforcement composites exhibiting approximately the same RVE size as those with 15% vol. reinforcement. This reduction of the RVE size can be explained by the fact that 25% vol. reinforcement is very close to the jamming limit of the distribution, therefore the linear elastic reinforcement forms a quasi continuous stiff network in the composite which limits the development of plastic strain concentrations. On the other hand in the composite with 20% vol. reinforcement the particles are not sufficiently packed to constrain plastic strain development. Overall, the estimated RVE size for high reinforcement volume fractions (15% to 25%) falls in the range of $10 < \xi < 20$, so approximately two to four times larger than the size of the RVE of elastic particle reinforced composites.

The results relative to the elastoplastic composites (figure 5) show that while the composition proves to have a very marked influence on the RVE size, the same can-

not be said for the hardening coefficient. The difference in the RVE size between the elastic perfectly plastic composite, h0 and that with the largest hardening, h2, is negligible, with the composites with perfectly plastic matrices having slightly larger RVEs (figure 5). Since the hardening range considered herein is wide, these results are likely to apply to a wide range of elastoplastic particle-reinforced composites and in particular to most of the PRMMC of technological interest. The same conclusion can be drawn for the elastoviscoplastic composites (figure 6), which under constant strain rate can be assimilated to elastic perfectly plastic materials: the estimated RVE sizes for $n = 4$ and $n = 8$ are very similar. Moreover, the considered range of stress exponents $4 \leq n \leq 8$ covers the majority of engineering materials, to which the present results apply.

The assessment of the small influence of constitutive parameters on the RVE size leads to the conclusion that the main parameter that determines it for an elastoplastic or elastoviscoplastic composite is the amount of plastic deformation developed in the matrix material. Note that the macroscopic plastic strain is an indicator of the average plastic strain in the material but it is not the volume average of the actual plastic strain in the matrix material (Suquet, 1985). If the results of the RVE sizes for the two mechanical behaviours are compared it can be noted that the RVE sizes at corresponding values of normalised strain are comparable. The curves in figures 5 and 6 can be used to have estimates of the RVE size for elastoplastic and elastoviscoplastic composites in the considered range of compositions with two caveats: 1) normalised strain values can correspond to very different levels of actual strain therefore the compatibility with the small strain assumption has to be verified, in particular it is recommended that the macroscopic strain is not larger than 5%, 2) the curves are representative of uniaxial monotonic loading and therefore have to be used with extreme caution when different loading histories are considered.

3.4 Stress-strain curve predictions

Two sets of normalized stress strain curves for representative elastoplastic and elastoviscoplastic composites are summarized in figures 7 and 8, respectively. The curves were obtained from models with $\xi = 13.9$ therefore they are plotted up to the maximum strain level at which the volume is representative. Note that the caveats for the employment of the RVE size curves (figures 5 and 6) hold for these stress-strain curves as well, in particular the macroscopic strain should not exceed 5% to satisfy the small strain assumption used in the FE models.

4 Summary and Conclusions

In this work, a large scale parametric study was carried out to assess the RVE size of elastoplastic and elastoviscoplastic particle-reinforced composites with a ran-

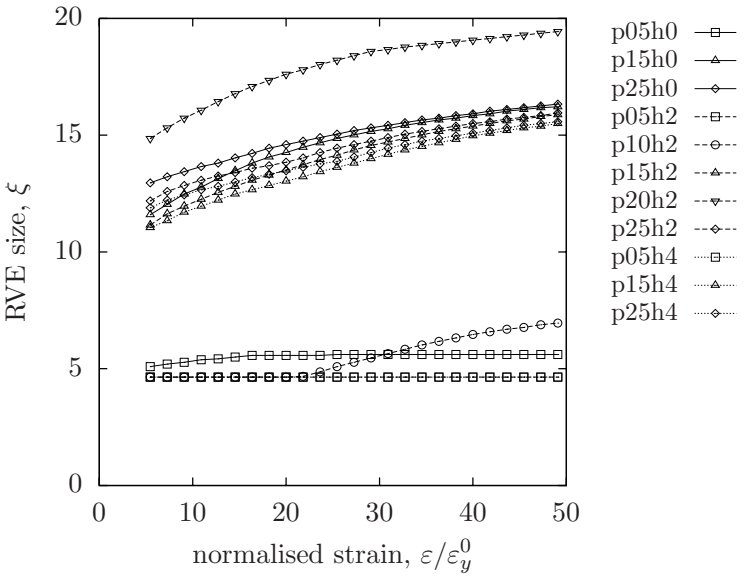

Figure 5: RVE size for elastoplastic composites. The hardening coefficient has a small influence on the RVE size compared to the reinforcement volume fraction and the strain level.

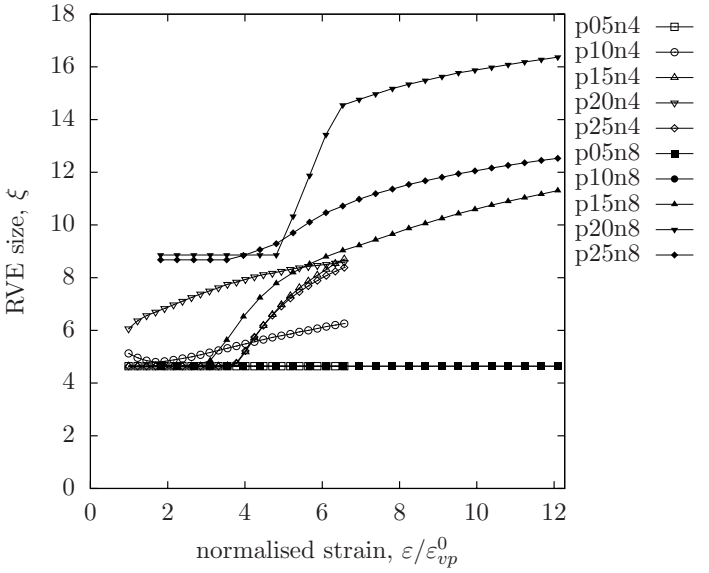

Figure 6: RVE size for elastoviscoplastic composites. The creep exponent has a small influence on the RVE size compared to the reinforcement volume fraction and the strain level.

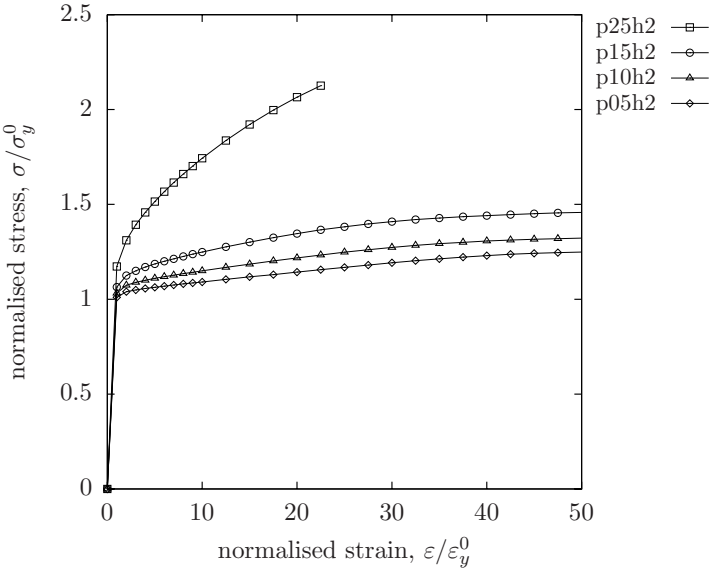

Figure 7: Non dimensional stress-strain curves for elastoplastic composites.

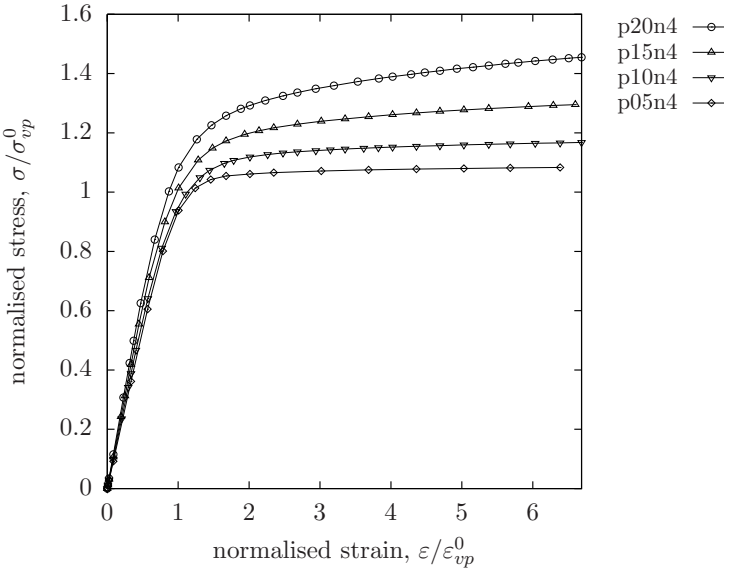

Figure 8: Non dimensional stress-strain curves for elastoviscoplastic composites.

dom microstructure. Reinforcement volume fractions up to 25% were considered. The range of values of the constitutive parameters of the base materials covers the majority of particle-reinforced metal matrix composites used in applications. Four different sets of uniform boundary conditions were employed: kinematic, static and two different types of mixed boundary conditions. The respective results were compared to evaluate their influence on the effective response. The two types of mixed uniform boundary conditions resulted the most appropriate since they lead to the same stress-strain response. Purely static boundary conditions resulted to be inappropriate because of premature plastic strain localization while kinematic boundary conditions lead to an overestimation of the stiffness of the composite material and therefore can be regarded as an upper estimate. A mesh convergence study showed that the convergence of the mesoscale model towards the RVE was not affected by the mesh refinement, nevertheless the level of mesh refinement is of key importance to obtain quantitative predictions of the macroscopic response of the material. The physical size of the RVE was estimated for each material behavior by taking the largest mesoscale model as a reference and constructing an error function depending on both model size and on the applied strain and then estimating the size corresponding to a maximum error of 2%. The RVE size proved to mostly depend on the volume fraction of reinforcement and on the accumulated plastic strain; on the contrary the material properties resulted to have a small influence on it. The estimates of the RVE size provided herein are instrumental to both numerical and experimental mechanics. For experiments, the RVE size estimates can be applied, for example, to evaluate the minimum size of a test specimen to obtain representative results while for numerical homogenization and multiscale modeling, the RVE size is the main parameter that determines the transition of scale between mesoscale microstructural models and macroscopic models, in which the response of a composite is described in terms of effective properties.

References

Böhm, H.J.; Han, W. (2001): Comparison between three-dimensional and two-dimensional multi-particle unit cell models for particle reinforced metal matrix composites. *Modelling and Simulation in Materials Science and Engineering*, vol. 9, pp. 47–65.

Böhm, H.J.; Han, W.; Eckschlager, A. (2004): Multi-inclusion unit cell studies of reinforcement stresses and particle failure in discontinuously reinforced ductile matrix composites. *CMES: Computer Modeling in Engineering & Sciences*, vol. 5, pp. 5–20.

Du, X.; Khisaeva, Z.; Li, W.; Ostoja-Starzewski, M. (2007): Comparisons of the

size of representative volume element in elastic, plastic, thermoelastic, and permeable random microstructures. *International Journal for Multiscale Computational Engineering*, vol. 5, pp. 73–82.

Drugan, W.J.; Willis, J.R. (1996): A micromechanics-based nonlocal constitutive equation and estimates of representative volume element size for elastic composites. *Journal of the Mechanics and Physics of Solids*, vol. 44, pp. 497–524.

Galli, M.; Janczak-Rusch, J.; Botsis, J. (2006): Relief of the residual stresses in ceramic-metal joints by a layered braze structure. *Advanced Engineering Materials*, vol. 8, pp. 197–201.

Galli, M.; Botsis, J.; Janczak-Rusch, J. (2008): An elastoplastic three-dimensional homogenization model for particle reinforced composites. *Computational Materials Science*, vol. 41, pp. 312–321.

Gitman, I.M.; Askes, H.; Sluys L.J. (2007): Representative Volume: Existence and Size Determination. *Engineering Fracture Mechanics*, vol. 74, pp. 2518–2534.

Gonzalez C.; Segurado, J.; LLorca, J. (2004): Numerical simulation of elasto-plastic deformation of composites: evolution of stress microfields and implications for homogenization models. *Journal of the Mechanics and Physics of Solids*, vol. 52, pp. 1573–1593.

Huet C. (1997): An integrated micromechanics and statistical continuum thermodynamics approach for studying the fracture behaviour of microcracked heterogeneous materials with delayed response. *Engineering Fracture Mechanics*, vol. 58, pp. 459–556.

Jiang, M.; Ostoja-Starzewski, M.; Jasiuk, I. (2001): Scale-dependent bounds on effective elastoplastic response of random composites. *Journal of the Mechanics and Physics of Solids*, vol. 49, pp. 655–673.

Li, W.; Ostoja-Starzewski, M. (2006): Yield of random elasto-plastic materials. *Journal of Mechanics of Materials and Structures*, vol. 1, pp. 1055–1073.

McDowell, D.L. (2010): A perspective on trends in multiscale plasticity. *International Journal of Plasticity*, vol. 26, pp. 1280–1309.

Nemat-Nasser, S.; Hori, M. (1993): *Micromechanics: Overall Properties of Heterogeneous Materials*, North-Holland.

Ostoja-Starzewski, M. (2005): Scale effects in plasticity of random media: status and challenges. *International Journal of Plasticity*, vol. 21, pp. 1119–1160.

Ostoja-Starzewski, M. (2008): *Microstructural Randomness and Scaling in Mechanics of Materials*, Chapman & Hall/CRC Press..

Pahr, D.H.; Zysset, P.K. (2008): Influence of boundary conditions on computed apparent elastic properties of cancellous bone. *Biomechanics and modeling in mechanobiology*, vol. 7, pp. 463–476.

Pahr, D.H.; Böhm, H.J. (2008): Assessment of Mixed Uniform Boundary Conditions for Predicting the Mechanical Behavior of Elastic and Inelastic Discontinuously Reinforced Composites. *CMES: Computer Modeling in Engineering & Sciences*, vol. 34, pp. 117–136.

Pierard, O.; LLorca, J.; Segurado, J.; Doghri, I. (2007): Micromechanics of particle-reinforced elasto-viscoplastic composites: Finite element simulations versus affine homogenization. *International Journal of Plasticity*, vol. 23, pp. 1041–1060.

Segurado, J.; Gonzalez C.; LLorca, J. (2003): A numerical investigation of the effect of particle clustering on the mechanical properties of composites. *Acta Materialia*, vol. 51, pp. 2355–2369.

Segurado, J.; LLorca, J. (2006): Computational micromechanics of composites: The effect of particle spatial distribution. *Mechanics of Materials*, vol. 38, pp. 873–883.

Shabana, Y.M.; Noda, N. (2002): Thermo-elasto-plastic stresses of functionally graded material plate with a substrate and a coating. *Journal of Thermal Stresses*, vol. 25, pp. 1133–1146.

Si, H. (2009): *TetGen: A Quality Tetrahedral Mesh Generator and Three-Dimensional Delaunay Triangulator, Version 1.4*.

Sivasubramaniam, V.; Galli M.; Cugnoni, J.; Janczak-Rusch, J.; Botsis, J. (2009): A Study of the Shear Response of a Lead-Free Composite Solder by Experimental and Homogenization Techniques. *Mechanics of Materials*, vol. 38, pp. 2122–2131.

Suquet, P.M. (1985): Elements of Homogenization for Inelastic Solid Mechanics. *Lecture Notes in Physics*, vol. 272, pp. 194–278.

van der Sluis, O.; Schreurs P.J.G.; Brekelmans, W.A.M.; Meijer, H.E.H. (2000): Overall behaviour of heterogeneous elastoviscoplastic materials: effect of microstructural modelling. *Mechanics of Materials*, vol. 32, pp. 449–462.

CMES: Computer Modeling in Engineering & Sciences

ISSN : 1526-1492 (Print); 1526-1506 (Online)

Journal website:
http://www.techscience.com/cmes/

Manuscript submission
http://submission.techscience.com

Published by
Tech Science Press
5805 State Bridge Rd, Suite G108
Duluth, GA 30097-8220, USA

Phone (+1) 678-392-3292
Fax (+1) 678-922-2259
Email: sale@techscience.com
Website: http://www.techscience.com
Subscription: http://order.techscience.com

CMES is Indexed & Abstracted in
Applied Mechanics Reviews; Cambridge Scientific Abstracts (Aerospace and High Technology; Materials Sciences & Engineering; and Computer & Information Systems Abstracts Database); CompuMath Citation Index; Current Contents: Engineering, Computing & Technology; Engineering Index (Compendex); INSPEC Databases; Mathematical Reviews; MathSci Net; Mechanics; Science Alert; Science Citation Index; Science Navigator; Zentralblatt fur Mathematik.